$S=\frac{1}{2}$ antiferromagnetic finite chains effectively isolated by frustration: $CuCl_2$-intercalated graphite

D. G. Rancourt,* C. Meschi, and S. Flandrois
Centre de Recherche Paul Pascal, Domaine Universitaire, 33405 Talence, France
(Received 29 July 1985)

We have measured the static susceptibility of nominal stage-2 $CuCl_2$-graphite intercalation compounds prepared from four different host graphites (highly oriented pyrolitic graphite, natural graphite crystals, and graphite fibers heat treated at 2500 and 3290 °C). The susceptibility and its anisotropy both contain a $1/T$ component which is shown to be due to finite-size effects and which, when removed from the data, reveals a bulklike behavior that closely corresponds to the pristine behavior for $T>50$ K. The behavior at lower temperatures is more complicated but is entirely consistent with an intercalate-island diameter of $d_{isl}\simeq 100$ Å, leading to a distribution of finite isolated quasi-Heisenberg antiferromagnetic chains of $S=\frac{1}{2}$ Cu^{2+} ions.

I. INTRODUCTION

Investigations of magnetic graphite-intercalation compounds (GIC's) have been motivated by the hope of observing low-dimensional behavior. Nevertheless, model systems have not yet been unambiguously identified. Consider the first-row transition-metal dichlorides which have been intercalated into graphite; MCl_2 with $M=$Mn, Co, Ni, and Cu. They are layered compounds of stacked octahedra with antiferromagnetic ($M=$Mn, Cu) or ferromagnetic ($M=$Co, Ni) near-neighbor in-layer coupling. Interlayer coupling causes the three-dimensional (3D) magnetic ordering temperatures to be, respectively, 1.9, 24, 50, and 24 K, for $M=$Mn, Co, Ni, and Cu. Since in a first approximation the pristine layers intercalate "as is," it was hoped that the GIC's which are formed would be more and more ideal two-dimensional systems as the stage of the compound is increased. One major experimental fact must, however, be taken into account—the islandic in-plane structure of the intercalant.[1]

We have recently shown[2] that in the ferromagnetic-type compounds ($M=$Co, Ni), the existence of islands changes what was thought to be an interesting problem in low-dimensional magnetism into a not less interesting problem of superferromagnetism. On the other hand, the antiferromagnetic-type compounds ($M=$Mn, Cu) are not expected to exhibit the same super-moment magnetism since the net islandic moments will be much smaller and $MnCl_2$ GIC does, in fact, have a quantitatively different behavior.[3] We were motivated to see how the magnetism of $CuCl_2$ GIC compares to that of the three other compounds and to that of the pristine material—especially since $CuCl_2$ itself already displays one-dimensional behavior.[4]

In this paper, we have performed magnetization measurements, in fields up to 60 kG and at temperatures between 1.9 and 300 K, on nominal stage-2 $CuCl_2$ GIC samples which were prepared with four different host graphites. The superconducting quantum interference device (SQUID) magnetometer used permitted measurements on individual crystals and very small highly oriented pyrolytic graphite (HOPG) samples such that relatively precise anisotropy measurements could be made.

All our measurements can be understood in terms of isolated finite-chain segments of $S=\frac{1}{2}$ Cu^{2+} ions which have near-neighbor antiferromagnetic coupling. The effective Hamiltonian contains a significant anisotropy term whose effects are unambiguously recognized. 3D ordering probably does not occur down to 1.9 K thereby classifying stage-2 $CuCl_2$ GIC as an excellent model system ($k_BT_c/|J|<0.03$) for studying finite ($N\approx 3$–60) one-dimensional $S=\frac{1}{2}$ antiferromagnetic chains. A detailed comparison with the pristine material is made and the "finite-size effects" are found to have a large and systematic dependence on the type of host graphite.

II. EXPERIMENTAL

Intercalation of $CuCl_2$ into graphite has been known for some time.[5] Stage-2 compounds can be obtained but the stage purity is highly sensitive to the nature of the graphite and its texture. Large graphite flakes and HOPG samples are particularly difficult to intercalate reproducibly compared to, for example, graphite powder.

In our study, four types of host materials were used: natural graphite crystals from Madagascar (roughly, $2\times 2\times 0.3$ mm^3), thin strips (roughly, $3\times 1\times 0.2$ mm^3) of HOPG, and two pitch-based carbon fibers (roughly, 1 cm long and 10 μm in diameter) from Union Carbide heat treated at, respectively, 2500 °C and 3290 °C. In the fibers, the graphite planes are parallel to the fiber axis and are disposed radially about the core.

The compounds were prepared by heating a mixture of graphite, $CuCl_2$ powder, and chlorine gas, in a sealed pyrex tube at around 500 °C during several days. After reaction, the product was washed with dilute HCl to remove the excess $CuCl_2$. The stage was determined by x-ray diffraction using Cu $K\alpha$ radiation. Chemical analysis was

performed on the natural graphite samples only; samples were oxidized in a Parr bomb, then chlorine and copper were analyzed by titration. In the case of HOPG and carbon fibers, the stoichiometry of the intercalated materials was estimated from weight-uptake measurements.

Although most of the experiments led to a mixture of stages, we were able to obtain quasipure stage-2 compounds with the natural graphite crystals and with the HOPG material. In such cases the stoichiometry was $C_{10}CuCl_{2.2}$. All of the natural graphite crystal based and HOPG based samples studied in this paper were prepared together in the same successful intercalation experiment and are hereafter referred to, respectively, as C-type and HOPG—type compounds. Figure 1 shows a typical x-ray spectrum for one C-type crystal. The (00l) reflections corresponding to the stage-2 spacing of 12.72 Å are indicated and a bump corresponding to a small amount (<1—2%) of infinite stage (i.e., graphite) can also be seen.

All of the samples based on the fibers heat treated at 3290 °C were again taken from a single preparation and are hereafter referred to as FA-type compounds. The stoichiometry was $C_{12}CuCl_{2.2}$—admitting the same chlorine excess as in the C-type materials. The samples based on fibers heat treated at 2500 °C are taken from an intercalation which distinguished itself by a surprisingly large weight uptake and are again seen to be mostly stage 2. These are hereafter referred to as FS-type samples.

The magnetization was measured using a S.H.E. Corp. variable temperature SQUID susceptometer. The samples were varnished onto a cotton thread and lowered into the vertical applied field. For C-type samples, when four crystals were used, these were varnished parallel to each other and such that they sandwiched the thread. For the measurements with the field perpendicular to the carbon planes, the samples were suspended using a rigid pure copper wire whose near-negligible magnetism was subsequently removed from the measured data. In that case, the misalignment from the horizontal was at most 2°—3°. The fiber samples typically contained 1000—2000 individual 1-cm-long fibers varnished together with their axes parallel to the supporting thread and to the applied field.

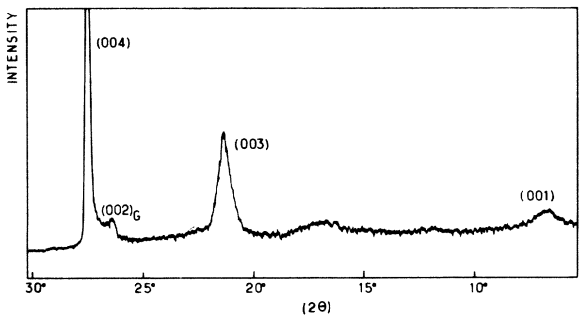

FIG. 1. X-ray diffraction pattern for one crystal of C-type $CuCl_2$ GIC. The (00l) lines correspond to stage 2. $(002)_G$ corresponds to the (002) reflection of graphite.

III. STRUCTURE AND SUSCEPTIBILITY: PRISTINE $CuCl_2$

Pristine $CuCl_2$ has a monoclinic crystal structure[6] with a bimolecular unit cell whose parameters are

$$a = 6.70 \text{ Å},$$

$$b = 3.30 \text{ Å},$$

$$c = 6.85 \text{ Å},$$

and

$$\beta = 121°,$$

as shown in Fig. 2. Each Cu^{2+} ion has four near-chloride ions at 2.48 Å and two next-near-chloride ions at 2.90 Å. Each Cu^{2+} ion is therefore surrounded by six chloride ions at the corners of a distorted octahedron [see Fig. 2(c)]. The octahedral building blocks are stacked such that the metal ions are linked together in linear chains which are parallel to the b direction and which have an intrachain metal-metal distance, d_1, of 3.30 Å ($=b$). The shortest metal-metal distance, d_2, to the first-nearest-neighbor (NN) chain is 3.80 Å and the corresponding distances, d_3 and d_4, to the second-nearest-neighbor (2NN)

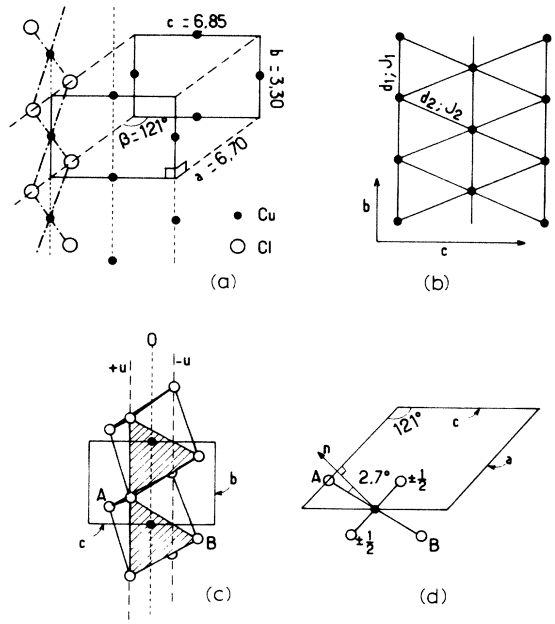

FIG. 2. Structure of pristine $CuCl_2$. (a) The bimolecular unit cell of $CuCl_2$ where three chains in the front (b-c) plane are indicated by the short-dashed lines and only the chlorine ions corresponding to the J_1 interactions for a single chain are shown. (b) The (b-c) plane in pristine $CuCl_2$. (c) Two Cu^{2+} ions from the (b-c) are shown with their respective chlorine octahedra. The shaded triangular faces are those which are seen to lie on the graphite planes in the intercalated compound. (d) Projection of the unit cell onto the (a-c) plane where only one octahedron is shown. The principal direction n, makes an angle of 2.7° with the main axis of the octahedron and is perpendicular to the (a-b) plane.

and third-nearest-neighbor (3NN) chains are, respectively, 5.975 Å and 6.70 Å ($=a$). d_1 and d_2 are distances within the same b-c plane whereas d_3 and d_4 are measured between two near b-c planes.

The chains behave as though they were magnetically isolated down to the 3D ordering temperature, T_c, of 23.9 K.[7] Above T_c, the magnetic susceptibility for powder samples shows a large rounded maximum at about 70 K and significant deviations from the high-temperature Curie-Weiss law starting at 550 K.[4] This behavior, for $T \gtrsim 50$ K, can be modeled equally well by Ising ($J=-70$ K) or Heisenberg ($J=-54.6$ K) infinite chains of antiferromagnetically coupled $S=\frac{1}{2}$ ions.

In order to account for the observed behavior, many have claimed that $d_2-d_1=0.50$ Å is a "large" distance and that, therefore, $|J_2|$ must much smaller than $|J_1|$. We do not agree. The two superexchange paths (each via one Cl ion) which are modeled by J_1 are not qualitatively different from the two superexchange paths which are modeled by J_2 and furthermore it is well known[8] that various superexchange bridges can lead to J's of the order of -500 K for inter-Cu^{2+} distances which are as large as 5.14 Å. The effective isolation of the chains above T_c is more likely due to magnetic frustration. The crucial point is that, admitting interactions only up to J_2 (with $J_1<0$ and $|J_1|>|J_2|$), the chains within a given (b-c) plane are translated with respect to each other by $d_1/2$ and are consequently exactly frustrated. Admitting interactions up to J_4, however, the chains are not frustrated with respect to chains in neighboring (b-c) planes and J_3 and J_4 are the main interactions which help (and determine) the transition to 3D order. The inter-(b-c) plane interactions can be modeled by a molecular field. Stout and Chisholm have shown[7] that such a molecular field, of the magnitude required to cause the transition at T_c, does not affect the susceptibility at $T>50$ K by more than a few percent.

Recently, much new information on the magnetism of pristine $CuCl_2$ has been obtained from measurements on single crystals.[4] The principal axes of the susceptibility tensor were found to be along b, a, and n—which is perpendicular to the (a-b) plane [see Fig. 2(d)]. The temperature dependence above approximately 50 K is essentially the same for the three principal susceptibilities and the following ratios can therefore be given:

$$\chi_a:\chi_c:\chi_n:\chi_b = 1000:929:899:860\ , \tag{1}$$

where $\chi_b^{\max}$ ($T=70$ K)$=2237\times10^{-6}$ emu/mole and χ_b ($T=292$ K)$=1191\times10^{-6}$ emu/mole (corrected for diamagnetism). We note, however, that the temperature, $T_{\max}$, at which $\chi^{\max}$ occurs is not the same for all directions and varies between 67 and 73 K—for example, $T_{\max}(b)-T_{\max}(a)\simeq+6$ K.

Near T_c and as T is lowered χ_b begins to drop rapidly whereas the susceptibilities perpendicular to the b direction remain roughly constant. This indicates that the local sublattice magnetization direction is along b. Also, a spin-flop transition is seen at $H_{SF}=41$ kG ($T=4.2$ K) and corresponds to a discontinuous step in the magnetization along b of $\Delta M_b=65$ emu/mole. The magnetizations measured along a, c, and n are continuous near H_{SF} and vary linearly up to 150 kG.

IV. STRUCTURE AND SUSCEPTIBILITY: INTERCALATED $CuCl_2$

In $CuCl_2$ GIC's the intercalant layers are essentially made up of (b-c) planes with $d_1'=3.34$ Å and $d_2'=3.82$ Å (Ref. 9) and we can therefore expect the interplane interactions (formerly J_3 and J_4) to be greatly reduced by the n graphite layers which separate the magnetic layers in an n-stage compound. Consequently, the 3D magnetic ordering temperature might be significantly lowered. An islandic structure in the plane of the intercalant will also affect the low-temperature magnetism. $NiCl_2$, $CoCl_2$, and $MoCl_5$ are known to have such a structure[1,10,11] with mean island diameters the order of 150—200 Å. Mean interisland distances are expected to be 10—15 Å in order to be consistent with the observed filling coefficients (typically 0.71) and chlorine excess (typically 10% or so).[1] We expect that $CuCl_2$ has a similar islandic structure. Also, the work of Hauw *et al.*[9] has shown to what extent a "stage-2" $CuCl_2$ GIC, which is well characterized by x rays is, on a local scale, actually a mixture of stage-0, -1, -2, and -3. Each stage domain is typically 2—6 intercalant layers thick (5—50 Å) and has a mean in-plane extension which is much greater (i.e., from the high resolution electron microscope pictures, we can estimate $\gg$500 Å). That work applies to compounds based on the same natural Madagascar graphite crystals which we have used as one of four of our host graphites. We expect the stage-domain structure to vary with the host graphite.

From the symmetry in a stage domain, the three principal susceptibilities can be given as follows: χ_c^i, in a direction perpendicular to the chains and in the plane of the intercalant; χ_b^i, in a direction parallel to the chains and in the plane of the intercalant; and $\chi_\perp^i$, in a direction perpendicular to both the chains and the intercalant layer. Note that two of the principal directions (c and $\perp$) are different, with respect to the octahedral directions, than in the pristine material. We refer to the average in-plane susceptibility for random in-plane orientations of the pieces of (b-c) planes which make up the intercalant layers as $\chi_{\|}^i \equiv (\chi_b^i+\chi_c^i)/2$. By analogy with the pristine material we can expect χ_c^i to be comparable to χ_c, χ_b^i to be comparable to χ_b, and $\chi_\perp^i$ to be comparable to its pristine analogue in the same direction, that is, $\chi_n\cos^2 59° + \chi_a\cos^2 31°$.

$\chi_\perp^i$ can be measured independently by probing in the direction perpendicular to the graphite layers in the HOPG— and C-type compounds. On the other hand, χ_c^i and χ_b^i cannot be measured independently and a measurement in the plane of the intercalant, for example, will lead to some average quantity such as $\chi_{\|}^i$.

In C-type $CuCl_2$ GIC there are three domains of b directions at 120° with respect to each other.[9] In addition, the supporting graphite itself can, as in the case of HOPG—type compounds, have various in-plane graphite lattice orientations. The FA- and FS-type compounds are interesting in that there seems to be a preferred intercalant orientation. Preliminary results[12] indicate that the direction $\mathbf{c}+\mathbf{b}$ is preferentially aligned along the fiber axis.

TABLE I. Average susceptibilities for different GIC sample types in various experimental geometries.

Sample type	Field direction	$\langle\chi\rangle$
FA, FS[a]	H|| fiber axis	$0.191\chi_b^i+0.809\chi_c^i$
FA, FS[a]	H⊥ fiber axis	$0.404\chi_b^i+0.096\chi_c^i+0.5\chi_\perp^i$
HOPG, C	H|| carbon plane	$\chi_{\|\|}^i=0.5\chi_b^i+0.5\chi_c^i$
HOPG, C	H⊥ carbon plane	$\chi_\perp^i$

[a]Assuming one domain of intercalate orientation with b+c parallel to fiber axis.

The measured susceptibilities can be derived in terms of the principal values by assuming that one stage domain dominates. Some results for various experimental geometries and supporting graphite materials (assuming ideal definition of the in-plane orientational order) are given in Table I.

V. RESULTS

The measured susceptibilities ($\chi_{\|}^i=M/H$) at 300-K range from 2.7×10^{-6} emu/g (for an FA-type sample) to 5.0×10^{-6} emu/g (for a C-type sample). By comparing with the known susceptibility of powdered $CuCl_2$ and having made the necessary diamagnetic corrections (0.440×10^{-6} emu/g for $C_{10}CuCl_{2.2}$ and 0.445×10^{-6} emu/g for $C_{12}CuCl_{2.2}$) this corresponds to filling coefficients which range from ≈0.4 to ≈0.9. Also, sample-to-sample variations in χ at 300 K, for a given intercalation and host graphite, were typically 10^{-6} emu/g.

All four sample types exhibit the same basic susceptibility versus temperature curve which, at first sight, appears to be simply a superposition of two contributions: (i) an "impurity" or "free-ion" contribution which can be expressed as A_f/T where A_f is a constant, and (ii) a "bulk-like" contribution, $\chi^{b1}(T)$, which closely corresponds to the measured susceptibility of $CuCl_2$. A few examples are shown in Figs. 3 and 4 where the "corrected data" is the resultant susceptibility, after subtraction of the A_f/T component, which we refer to as bulklike.

The total susceptibility is linear in $1/T$ to within 1% in the temperature range from 5 to 10 K and for fields $H\leq1$ kG. This enables the slope, A_f, of the line and its intercept, χ^0, to be determined with some precision. A_f is always the order of 10^{-4} emu K/g and has a systematic dependence on the sample type as shown in Fig. 5 which is a plot of A_f versus χ^0 for all the samples we have studied in sufficiently low fields. The sudden drop in A_f for the HOPG—type samples which is suggested by the dashed line may be due to the fact that the two smaller samples (0.24 and 0.36 mg as opposed to 1.07 mg) had to be measured in 5 kG fields rather than 1 kG.

The susceptibility at $T=1.9$ K and for $H\leq1$ kG is largely [$A_f/(1.9\text{ K})\ \chi^0\approx10$] due to the $1/T$ component and the magnetization at this temperature begins to saturate at fields of the order of 1 kG as shown in Fig. 6. The saturation values which can be estimated from graphs of M versus $1/H$ are $M_S\gtrsim1.33$ emu/g for the FA-type sample which was measured and $M_S\gtrsim2.3$ emu/g for the C-type sample. These values correspond, respectively, to $0.068\mu_B$ and $0.108\mu_B$ per assumed $C_{12}CuCl_{2.2}$ and $C_{10}CuCl_{2.2}$ molecules. For comparison, assuming that the A_f/T contribution to χ is due to free paramagnetic Cu^{2+} ions, then the A_f values (evaluated between 5 and 10 K

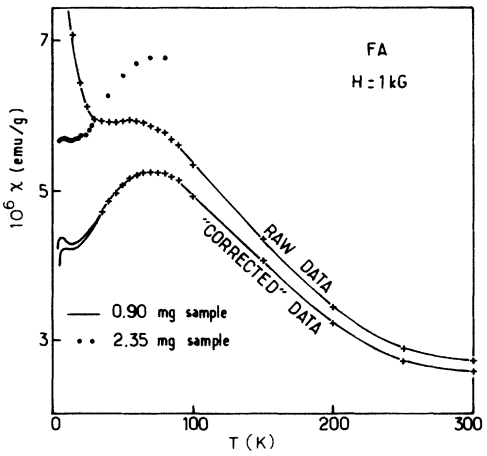

FIG. 3. Susceptibilities versus temperature for two FA-type samples at 1 kG applied along the fiber axis. Both the measured (raw) data and the extracted ("corrected") data are shown for the 0.90 mg sample and only the extracted data is given for the 2.35-mg sample. The two solid lines at low T and for the 0.90-mg sample bracket the allowed error in the resultant susceptibility given the error in A_f. The corresponding error in the 2.35-mg data is smaller than the diameter of the circles. The corrections for diamagnetism are not included.

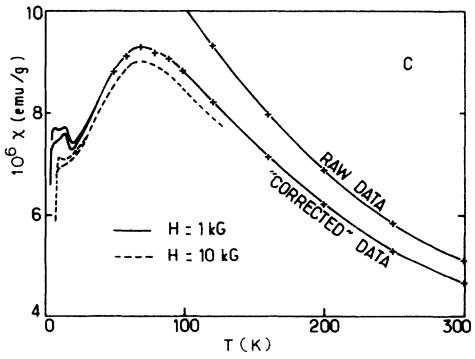

FIG. 4. Susceptibility versus temperature for a single C-type crystal at two fields applied in the plane. Only the extracted data is shown for the $H=10$ kG measurements where the same A_f, as obtained from the lower field ($H=1$ kG) measurements was used. The diamagnetic corrections are not made.

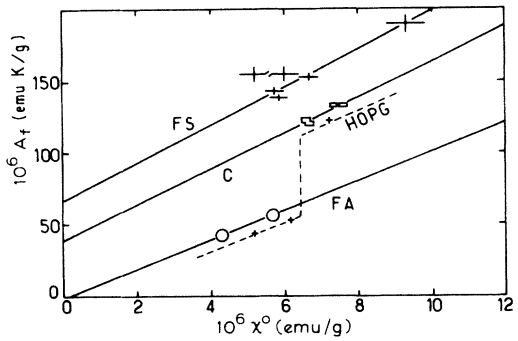

FIG. 5. A_f vs χ^0 for all samples measured in sufficiently low fields for A_f to be extractable at low temperatures. The measured data could be fitted with $\chi=A_f/T+\chi^0$ to within 1% in the temperature range 5 to 10 K and for $H\leq 1$ kG. The errors are (i) within the width of the solid line for the FA-type samples; (ii) shown by rectangles for the C-type samples; (iii) shown by the crosses for the FS-type samples; and (iv) are somewhat larger than the crosses which correspond to the HOPG—type samples. The field was in the intercalant plane for both C-type and HOPG—type samples and parallel to the fiber axis for the FA- and FS-type samples.

and at $H=1$ kG) for the same samples correspond, respectively, to $0.027\mu_B$ and $0.077\mu_B$ per assumed $C_{12}CuCl_{2.2}$ and $C_{10}CuCl_{2.2}$ molecules where the relevant relation is (μ_B's per molecule) equal to $3k_BM_{\rm mol}A_f/p^2\mu_B^2N_A$. $p=1.9$ is the effective Bohr magneton number for Cu^{2+} ions and $M_{\rm mol}$ is the molar mass.

The magnetization versus field measurements showed no discontinuous step in M near the 41-kG spin-flop field of the pristine material to within a possible error of 0.01 emu/g. The step would correspond to $\Delta M\approx 65$ emu/mol/$2M_{\rm mol}=0.13$ emu/g if the "bulk" contribution to χ was pristinelike with a 3D ordering temperature $T_c>1.9$ K.

The inset of Fig. 6 shows the hysteresis in the M versus H curve for the cycle 0 kG→60 kG→0 kG at $T=1.9$ K. It is then possible to measure the resultant remanent magnetization reversibly as a function of T up to temperatures

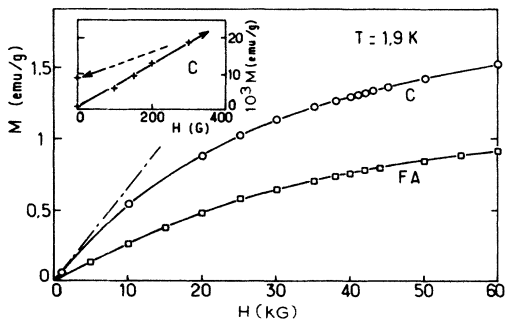

FIG. 6. Magnetization versus field strength for two samples at $T=1.9$ K. H is in the plane for the C-type sample and is parallel to the fiber axis for the FA-type sample. The low field ($H<1$ kG) linear dependence for the C-type sample is shown by the dot-dashed line. The inset shows the hysteresis loop (0 kG→60 kG→0 kG) for the same C-type sample at $T=1.9$ K.

of the order of 100 K. The result is the same as if the sample was zero-field cooled and then measured in some effective field which is typically 140—360 G. Notably, the zero-field value, after cooling in a strong field (H_c), of the ratio A_f/χ^0 is the same as in zero-field-cooled measurements with fields up to 1 kG applied in the same direction as H_c.

An important characteristic of the A_f/T contribution is its anisotropy. In the C-type sample which we studied in detail, the A_f value measured with the field perpendicular to the graphite planes, $A_f^{\perp}$, is surprisingly different from the value, $A_f^{\parallel}$, for an in-plane field; $A_f^{\parallel}-A_f^{\perp}=+(19.1\pm1.8)\times10^{-6}$ emu K/g. Some results for this sample are shown in Fig. 7. The anisotropy in the bulklike contribution is of opposite sign and dominates at higher temperatures. At low temperatures and for the same sample, we have $\chi_{\parallel}^0-\chi_{\perp}^0=-(1.18\pm0.20)\times10^{-6}$ emu/g such that the graphite plane is the plane of easy directions at low T and up to $T=16\pm4$ K, at which temperature the anisotropy is zero and above which the easy direction is perpendicular to the graphite planes. We note that the anisotropies in the effective g values for the two contributions to χ have the same magnitude (within error) but opposite sign and are given, respectively, by

$$-\Delta p=p_{\parallel}-p_{\perp}/\langle p\rangle=A_f^{\parallel}-A_f^{\perp}/A_f^{\parallel}+A_f^{\perp}=+0.085\pm0.004 \quad (2)$$

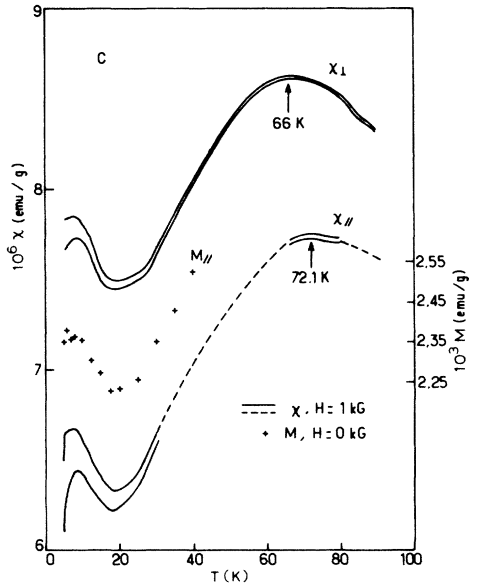

FIG. 7. Extracted susceptibility ($\chi_{\rm measured}-A_f/T$) versus temperature for two field directions with the same C-type sample. $\chi_\perp$ is for H perpendicular to the planes and $\chi_{||}$ is for in-plane measurements. The two solid lines for a given field direction bracket the possible values of the extracted susceptibilities given the errors in A_f. The dashed line is an extrapolation for missing data, otherwise, data points at every 2.5 K were taken for $T>12$ K and at every 1 K for $T<12$ K. Also shown is the extracted remanent magnetization ($M_{||}$) measured along the plane (on the same sample) after a cooling field of 60 kG was applied in that direction at $T=40$ K.

and

$$-\Delta g^0=g_{||}-g_{\perp}/\langle g\rangle=\chi^0_{||}-\chi^0_{\perp}/\chi^0_{||}+\chi^0_{\perp}=-0.082\pm0.007\ , \tag{3}$$

where, if the A_f/T part were due to free Cu^{2+} ions, we would expect $\langle p\rangle=p=1.9$.

We now describe the bulklike contribution in more detail. It is closely analogous to the susceptibility which is measured in pure $CuCl_2$ and exhibits a broad maximum at the same temperature, within a few degrees, as in the pristine material. The maximum occurs at 72.1 K for measurements parallel to the plane and at 66 K when the applied field is perpendicular to the graphite layers.

At lower temperatures, where the errors due to the subtraction of the linear-in-$1/T$ component are largest, the bulklike contributions for many samples exhibit an anomaly (see Fig. 7) which can be described as follows. When the anomaly is sufficiently well defined it consists of a "bump" which begins to rise near 18 ± 2 K, has its maximum value near 8.5 ± 1 K, and then has a rapid and sudden decrease at some lower temperature of the order of 4 ± 2 K. Most importantly, the shape and magnitude of the anomaly are very sensitive (as seen in Figs. 3, 4, and 7) to the slope A_f—even within the error in A_f which is typically 2%. From Fig. 7 we can estimate the ratio of the magnitude of the anomaly to the maximum susceptibility to be 0.045 ± 0.005 for the parallel direction and 0.041 ± 0.003 for the perpendicular direction. One should be more wary of these numbers than the errors we have given seem to indicate. These errors are essentially due to the errors in A_f when A_f is obtained from χ in the interval 5 to 10 K but this interval may correspond to one where the nonbulklike contribution does not have a truly $1/T$ behavior as shall be explained in Sec. VI. We shall, in fact, show that the anomaly is an artifact of our extraction procedure and that such an artifact is consistent with finite-size effects due to intercalant-island diameters of the order of 100 Å.

VI. DISCUSSION

Although the geometry is less transparent than in the present case of intercalated $CuCl_2$ (b-c) planes, it has recently been shown by a Monte Carlo simulation[13] that 1D-like behavior of the susceptibility (and specific heat) can occur within a confined temperature range in a 3D frustrated lattice. Our results indicate that the frustrated 2D lattice which is shown in Fig. 2(b) is equivalent, with regards to the magnetic susceptibility, to its analogue with $J_2=0$ (i.e., that the frustration effectively isolates the chains whose ions are coupled by J_1) and this is our primary assumption in the following discussion.

First of all, it is clear that a finite antiferromagnetic chain with an odd number of ions can lead to a low-temperature susceptibility which goes as $1/T$. This has been shown[14] for Heisenberg ($S=\frac{1}{2}$) chains and can be demonstrated for the Ising ($S=\frac{1}{2}$) and classical Heisenberg ($S=\infty$) finite chains as follows. The exact Ising chain solution ($J_x=J_y=0$, H in z direction) is

$$\chi_{I(||z)}=Ng^2\mu_B^2\exp(J_z/k_BT)\times[1-(-\tanh K)^N]/4k_BT[1+(-\tanh K)^N]\ , \tag{4}$$

where N is the number of ions and $K=|J_z|/2k_BT$. The low-temperature expansion for odd N yields

$$\chi_{I(||z)}(N=\text{odd})\simeq g^2\mu_B^2(1-Ne^{-2K})/4k_BT\ . \tag{5}$$

The correction to the $1/T$ term decays rapidly as $T\to0$ K and is proportional to N. For even N at low T we obtain $\chi_{I(||z)}$ $(N=\text{even})=g^2\mu_B^2N^2e^{-4K}/4k_BT$. By comparison, the contribution to paramagnetic susceptibility from a single ($S=\frac{1}{2}$) spin is $S(S+1)g^2\mu_B^2/3k_BT=g^2\mu_B^2/4k_BT$. Now consider the classical limit ($S\to\infty$) for finite Heisenberg chains—the exact solution is[15]

$$\chi_{\text{cl}}=\chi^0_{\text{cl}}\{[N(1+U)/(1-U)]-[2U(1-U^N)/(1-U)^2]\}\ , \tag{6}$$

where $U=1/K-\coth K$ and $\chi^0_{\text{cl}}=g^2\mu_B^2/12|J|$. This leads to low temperature expansions which, to second order in $1/K$, are given by:

$$\chi_{\text{cl}}(N=\text{odd})=\chi^0_{\text{cl}}|J|\{1+[N(N-1)/4-1]/K^2\}/k_BT \tag{7}$$

and

$$\chi_{\text{cl}}(N=\text{even})=N\chi^0_{\text{cl}}[2-(N-1)k_BT/|J|]\ , \tag{8}$$

where $|J|$ is related to the temperature at which the maximum susceptibility, $\chi^{\max}_{\text{cl}}$ occurs by $k_BT_{\max}/|J|=0.2382$ and also $\chi^{\max}_{\text{cl}}/\chi^0_{\text{cl}}=1.2045$.

Equations (5) and (7) suggest that short odd antiferromagnetic chains contribute a $1/T$ component to χ irrespective of the particular effective Hamiltonian under consideration (i.e., whether Ising, XY, Heisenberg or some mixture of these) and that the contribution from one odd chain is equivalent to a contribution from a single ion whose g-factor anisotropy is determined by the underlying chain Hamiltonian and whose susceptibility in a given direction can be expressed as

$$\chi(N=\text{odd})\simeq\alpha g^2\mu_B^2(1+\epsilon)/k_BT\ , \tag{9}$$

where α is of the order of $\frac{1}{4}$. Assuming Eq. (9), the experimental values of μ_B's per Cu^{2+} ion, as deduced from the magnitude of the $1/T$ component, A_f, are consistent with the number of odd chains per Cu^{2+} ion when the circular island diameter is the order of 50–100 Å as can be seen from Table II. We now show that the low-temperature Curie-type tail can unambiguously be attributed to odd chains rather than isolated ions since such chains yield a low-temperature anomaly identical to the observed anomaly. The curious behavior of the effective g-factor anisotropy [i.e., roughly the same magnitudes, opposite signs—recall Eqs. (2) and (3)] is also seen to be a consequence of finite chains.

We simulate the susceptibility for circular islands ($d_{\text{isl}}=50$–300 Å) using Eq. (6) and find that the low temperature χ does in fact have a close $1/T$ dependence. We extract a slope, A_{ch}, in the reduced temperature range $T/T_{\max}=0.071$ to 0.143 (i.e., 5 K/70 K to 10 K/70 K as

TABLE II. Spin counting with circular islands. d_{isl} represents circular island diameter; TNS, total number of spins in an island; NOC, number of odd chains; ALC, average chain length in spin numbers; MCL, maximum chain length in spin numbers; NOC/TNS, number of μ_B's per Cu^{2+} ion.

d_{isl} (Å)	TNS	NOC	ACL	MCL	NOC/TNS
50	170	7.5	11.7	15.0	0.044
100	680	15.1	23.6	29.9	0.022
200	2740	30.1	47.0	59.9	0.011
300	6160	45.2	70.0	89.8	0.0073

in the real system) and find that the error in A_{ch} is comparable to the experimental error in A_f. Furthermore, there is a systematic deviation from A_{ch}/T which is comparable to the observed systematic deviations from A_f/T at zero applied fields (high field cooled experiments) and in applied fields up to 1 kG. This suggests that the observed deviations are due to a chain-size distribution rather than saturation effects. When A_{ch}/T is removed from the simulated data, for various A_{ch} values within the "error," a low-temperature anomaly can be made to appear or disappear. If we maximize the amplitude of this anomaly it is seen to become very similar to the largest anomalies which are obtained from the measured data. This is illustrated in Fig. 8 for $d_{isl}=300$ Å. Typically, the ratio of the magnitude of the calculated anomaly to χ_{cl}^{max} is 0.03—0.06—in excellent agreement with the observed anomaly. The shape of the calculated anomaly is the same as that of the observed anomaly; a slower rise than subsequent decrease as T is lowered and a sudden and rapid drop on the low-T side (compare Figs. 8 and 7). Also, the reduced temperature (i.e., T/T_{max}) at which the maximum in the anomaly occurs is typically a factor of 4 lower than the observed value. That is, the anomaly

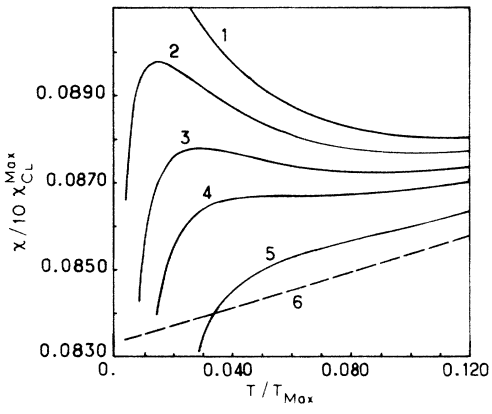

FIG. 8. Calculated extracted susceptibilities versus reduced temperature (T/T_{max}) assuming circular islands with $d_{isl}=300$ Å and using Eq. (7). The corresponding χ_{CL} in the limit $N\to\infty$ is shown by the dashed line (label 6). The labels 1—5 are related to values of $A_{ch}M_{mol}k_B/N_A g^2\mu_B^2$ as follows: 5.1×10^{-4} (label 1), 5.2×10^{-4} (label 2), 5.3×10^{-4} (label 3), 5.4×10^{-4} (label 4), and 5.6×10^{-4} (label 5).

would occur near 2 K instead of 8.5±1 K. This difference in position may be partly due to a distribution of island diameters or to ellipcal island shapes but it is probably mostly due to the assumed classical Hamiltonian. The difference can be expected to disappear for a more realistic (i.e., $S=\frac{1}{2}$) effective Hamiltonian since such a Hamiltonian (Ising, XY, or Heisenberg) has a relatively more constant χ at low temperatures and in the limit of large N. This cannot be verified since solutions for both even and odd arbitrary N ($N=3$—100 in particular) are not presently available for the $S=\frac{1}{2}$ Hamiltonians with all the field directions which are needed.

We now turn to the behavior of the anisotropies Δp and Δg^0. At first sight the change in sign is curious, since supposing that the anisotropies are due to a small uniaxial magnetocrystalline term of the form $D_a\sum_i (S_z^i)^2$ in an otherwise isotropic Heisenberg Hamiltonian, then D_a must have opposite signs for odd and even chains. Or, equivalently, the free-ion contribution to χ must correspond to ions in a different crystallographic site for which there is no experimental evidence.

In order to show that the observed anisotropies are consistent with finite chains we perform the following calculation. We search for a relation similar to Eq. (9) for effective Hamiltonians of the form

$$\mathcal{H}_{eff}=J_x\sum_{NN}S_x^iS_x^j+J_y\sum_{NN}S_y^iS_y^j+J_z\sum_{NN}S_z^iS_z^j+g\mu_BH\sum_i S_H^i\ , \tag{10}$$

where NN indicates summation over nearest neighbors only, in an effort to calculate α for various exchange constants and directions of applied field for the special case of the odd chains with $N=3$. The problem can be solved exactly for any Hamiltonian given by Eq. (10) and consists in diagonalizing a $2^3\times2^3$ matrix in order to obtain the eigenvalues of $\mathcal{H}_{eff}$. The low-temperature susceptibility is independent of whether the two end spins interact or not (i.e., of whether we have a closed ring or a line of three spins) and should be similar to that obtained from larger odd chains. Some values of α, which can be obtained in a manner suggested by Eq. (9), are as follows: Heisenberg ($J_x=J_y=J_z<0$) $\alpha_\perp=\alpha_{||}=\frac{5}{36}$; XY model ($J_x=J_y<0$, $J_z=0$) $\alpha_\perp=\frac{1}{36}$; Ising ($J_x=J_y=0$, $J_z<0$) $\alpha_{||}=\frac{1}{4}$, which is confirmed by Eq. (5), and $\alpha_\perp=T/360$. $\alpha_{||}$ refers to the configuration where the field is applied along the largest J direction (along x or y in the case of the XY model) and $\alpha_\perp$ refers to the configuration where the field is applied in the direction of the smallest J. Note that, in the Ising case, the odd chain perpendicular susceptibility is independent of T at low T. In fact, for arbitrary $\mathcal{H}_{eff}$, Eq. (9) is not obeyed, however, the low-temperature behavior can be expressed as

$$\chi(N=\text{odd})\simeq\alpha_{(\perp\text{ or }||)}g^2\mu_B^2(1/k_BT)^{m(\perp\text{ or }||)}\ , \tag{11}$$

where, in particular, $m_\perp=0$ in the Ising case and $m_\perp, m_{||}\simeq1$ for "near-Heisenberg" Hamiltonians. Eq. (11) deserves more attention as follows.

We redefine $\mathcal{H}_{eff}$ such that $J_x=J_y=J<0$ and $J_z=J+j$. The Heisenberg, Ising, and XY Hamiltonians

then correspond, respectively, to $j=0$, $j\to-\infty$ and $j=-J$. In the limit of small $|j|$, a calculated Δp, which corresponds to the measured value, can be defined as $\Delta p_c=(\alpha_\perp-\alpha_{||})/(\alpha_\perp+\alpha_{||})$ and is found to be always negative irrespective of the sign and magnitude of j. Also, as illustrated in Fig. 9, Δp_c is linear in $|j|$ near $j=0$ from which we obtain $|j|/|J|\simeq 0.0078\mp 0.0004$ for the Cu^{2+} chains in $CuCl_2$ GIC ($J=-54.6$).

The case of even N is more ambiguous since small even chains ($N=2$, for example) are not representative of larger even chains. All the available results on infinite chains, however, are consistent with $\Delta g^0>0$. It is therefore not unreasonable to expect that $\Delta g^0\simeq-\Delta p$ (as we find experimentally for $|j|\simeq 0.4$ K) if the bulklike contribution is mostly due to sufficiently long even chains.

Figure 10 shows the net measured anisotropy, $\chi^i_\perp-\chi^i_{||}$, as a function of temperature. The anisotropy in the bulklike contribution, $\chi^{b1}_\perp-\chi^{b1}_{||}$, and the calculated anisotropy, $\chi^{cp}_\perp-\chi^{cp}_{||}$, assuming that the octahedra have the same principal susceptibilities as in the pristine material are also shown. At high temperatures the χ^{b1} anisotropy follows the χ^{cp} anisotropy quite closely down to $T\simeq 50$ K at which point $\chi^{cp}_\perp-\chi^{cp}_{||}$ overshoots $\chi^{b1}_\perp-\chi^{b1}_{||}$ because of the phase transition at $T_c=23.9$ K in the pristine material. The χ^{b1} anisotropy is characteristic of antiferromagnetic chains with anisotropic Hamiltonians although, admittedly, the data is not inconsistent, within error, with a 3D ordering which could occur at $T<5$ K.

Finally, we discuss the possible meaning of Fig. 5. χ^0 is proportional to the number of Cu^{2+} ions per g which contribute a constant term to χ at low T. χ^0 is therefore mostly due to the large chains—especially those with even N. A_f is proportional to the number of odd chains per g. With δ-function distributions of island diameters, we expect the samples from a given intercalation to fall on a straight line which passes through the origin and whose slope depends only on d_{isl}. This is the case for the FA-type samples where the errors in χ^0 and A_f are smallest. Straight lines which pass through the origin can also be made, within the maximum errors, to pass through the points corresponding to the other sample types. The larger slopes $(\partial A_f/\partial\chi^0)$ would then correspond to much smaller island diameters. We prefer another interpretation since we do not believe that it is by accident that the best lines for all the intercalations have roughly the same slope. A nonzero positive A_f at $\chi^0=0$ (i.e., $A_f^0>0$) implies that, in the limit of zero filling coefficients and after we have removed all the islands, there remains a finite number of "free" ions and/or a finite number of odd chains and/or a certain number of ions in a second population of islands which have a much smaller diameter. This is consistent with the fact that the FS fibers were heat treated at a lower temperature than the FA fibers and therefore probably have a higher density of defects which may lead to a less homogeneous intercalation. The intercalation independent slope $(\partial A_f/\partial\chi^0\simeq 10$ K) is then understood to be a consequence of a large-island diameter ($d_{isl}\simeq 100$ Å) which is roughly the same irrespective of the particular host graphite used. There is, however, a discernible correlation between $\partial A_f/\partial\chi^0$ and A_f^0 (A_f at $\chi^0=0$) which can be expressed as $\partial A_f/\partial\chi^0\simeq(2\times 10^5$ g/emu$)\,A_f^0+10.1$ K and which suggests that the small-island (and/or odd-chain and/or free-ion) contribution is greater for samples which have a smaller large-island diameter.

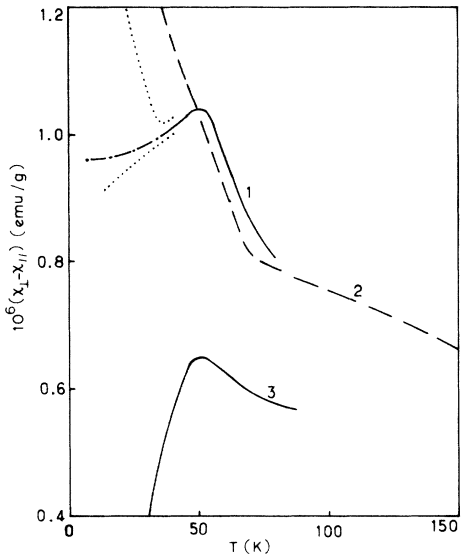

FIG. 10. Measured (curve 3), calculated (curve 2), and extracted (curve 1) magnetic anisotropies at $H=1$ kG and for the same C-type sample as in Fig. 7. The dotted lines bracket the possible error in curve 1 given the extraction procedure. The dot-dashed line represents data that would be consistent with infinite isolated chains. Curve 1 may be referred to as the anisotropy in the bulklike contribution to χ. The calculation which leads to curve 2 assumes that the octahedra have the same principal susceptibilities as in pristine $CuCl_2$.

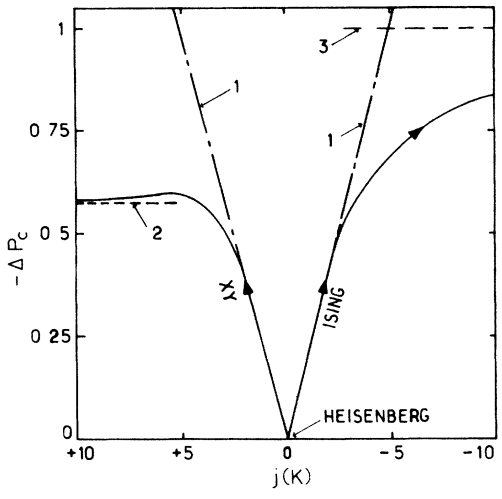

FIG. 9. The calculated effective g factor anisotropy, $-\Delta p_c$, in the free-ion—like low-temperature tail as a function of j for $J=-100$ K and $N=3$. Curve 1 shows the asymptotic behavior ($-\Delta p_c=|j|/5$) near $j=0$. Curve 2 shows the XY limit of $-\Delta p_c$ and curve 3 shows the Ising limit. The figure is "incomplete" in that it says nothing about the α values themselves or about the exponents $m_\perp$ and $m_{||}$ which are nearly equal to 1 in the region where curve 1 holds.

VII. CONCLUSION

The low field susceptibilities for all of the $CuCl_2$ GIC samples we have studied have two distinct contributions, $\chi^{b1}(T)$ and A_f/T, such that the total measured susceptibility as a function of temperature can be written as $\chi(T)=\chi^{b1}(T)+A_f/T$. The linear-in-$1/T$ term is attributed to finite chains with an odd number of spins and χ^{b1} is attributed to chains with large numbers of spins. The distinction is not "clear cut" since at low temperature mostly even chains contribute to χ^{b1} ($\simeq\chi^0$ at low T) whereas at higher temperatures both even and odd chains contribute to χ^{b1}. $\chi^{b1}(T)$ closely resembles the susceptibility of the pristine material and notably exhibits a large broad maximum at the same temperature of $T_{max}\simeq 70$ K and the same functional dependence on temperature for $T\gtrsim 50$ K. At low temperature χ^{b1} often exhibits an anomaly which, at first sight, might correspond to a genuine magnetic ordering phenomenon but which we show is an artifact arising from the finite chains.

The anisotropy measurements on a C-type sample lead to a total anisotropy which slowly rises as T is lowered, has a maximum of $+0.65\times 10^{-6}$ emu/g near 50 K, and then has a rapid decrease to become zero near 16 K and negative at lower temperatures. As with the susceptibility, this behavior of the anisotropy can be separated into two components: one which goes as $(A_f^{\perp}-A_f^{\parallel})/T$ and dominates at lower temperatures and another, $\chi_{\perp}^{b1}(T)-\chi_{\parallel}^{b1}(T)$, which closely follows the corresponding pristine anisotropy for $T>50$ K, diverges considerably from the pristine anisotropy for $T<50$ K, and is consistent with long antiferromagnetic chains at all temperatures. Both contributions to the anisotropy (and, in fact, all of our susceptibility data) can be understood to arise from a distribution of finite-chain lengths. Given a single effective near-Heisenberg Hamiltonian for all the chains, the measured anisotropy and susceptibility are then seen to be an immediate consequence of a chain length distribution which, in a circular island model, corresponds to $d_{isl}\simeq 100$ Å.

The anisotropy in the effective Hamiltonian is clearly demonstrated by two experimental facts—the existence of a magnetic anisotropy and the dependence of T_{max} on the orientation of the applied field. The anisotropic term in $\mathcal{H}_{eff}$ may be due to the next-nearest-neighbor interaction J_2 and it would be interesting to obtain the calculated effective Hamiltonian for the frustrated lattice of Fig. 2(b) by solving the lattice either exactly or by Monte Carlo.

Finally, the sample-to-sample and intercalation-to-intercalation (i.e., host-graphite—to—host-graphite) variations of A_f and χ^0, while not conclusive due to the large experimental errors in these quantities, suggest that (i) for a given host graphite and identical intercalation conditions, A_f is correlated to χ^0 in a manner consistent with the idea that the greater the filling coefficient, the greater the number of odd chains, (ii) the mean island diameter, which represents most of the ions, is roughly the same for all host graphites irrespective of the filling coefficient and of the particular conditions of intercalation, and (iii) an increased number of defects in the host graphite may represent a tendency for the formation of a second family of islands with considerably smaller diameters (i.e., a tendency towards an increased density of isolated "freelike" or "short-odd-chain-like" spins).

ACKNOWLEDGMENTS

One of us (D.G.R.) gratefully acknowledges the financial support of the Natural Sciences and Engineering Research Council of Canada.

*Present address: Kamerlingh Onnes Laboratorium, Der Rijksuniversitet, Nieuwsteeg 18, Postbus 9506, 2300 RA Leiden, Nederland.

[1]S. Flandrois, A. W. Hewat, C. Hauw, and R. H. Bragg, Synth. Met. 7, 305 (1983).

[2]D. G. Rancourt, J. Magn. Magn. Mater. (to be published).

[3]Y. Kimishiba, A. Furukawa, K. Koga, H. Nagano, and M. Suzuki, Proceedings of the Materials Research Society Conference on Graphite Intercalated Compounds (unpublished); O. Gonzalez, S. Flanders, A. Maaroufi, and J. Amiell, Solid State Commun. 51, 499 (1984).

[4]D. Billerey, thesis, Universite de Nancy I, Nancy, France, 1978; D. Billerey, C. Terrier, R. Mainard, M. Perrin, and J. Hubsch, Phys. Lett. 68A(2), 275 (1978); D. Billerey, C. Terrier, R. Mainard, N. Ciret, and A. J. Pointon, J. Magn. Magn. Mater. 30, 55 (1982), and references therein.

[5]W. Rudorf, E. Stumpp, N. Spriessler, and F. W. Siecke, Angew. Chem. Int. Ed. Engl., 2, 69 (1963).

[6]A. F. Wells, J. Chem. Soc. 1670 (1947).

[7]J. W. Stout and R. C. Chisholm, J. Chem. Phys. 36(4), 979 (1962).

[8]M. F. Charlot, M. Verdaguer, Y. Journaux, P. de Loth, and J. P. Daudey, Inorg. Chem. 23, 3802 (1984).

[9]C. Hauw, J. Gaultier, S. Flandrois, O. Gonzalez, D. Dorignac, and R. Jagut, Synth. Met. 7, 313 (1983).

[10]A. W. S. Johnson, Acta Crystallogr 23, 770 (1967).

[11]M. Elahy, M. Shayegan, K. Y. Szeto, and G. Dresselhauss, Synth. Met. 8, 35 (1983).

[12]C. Hauw, C. Meschi, and S. Flandrois (unpublished).

[13]O. Nagai, Y. Yamada, and H. T. Diep, Phys. Rev. B 32, 480 (1985).

[14]J. C. Bonner and M. E. Fisher, Phys. Rev. 135, A640 (1964).

[15]M. E. Fisher, Am. J. Phys. 32, 343 (1964).